Nuclear Materials and Energy 45 (2025) 102016

Contents lists available at ScienceDirect

Nuclear Materials and Energy

journal homepage: www.elsevier.com/locate/nme

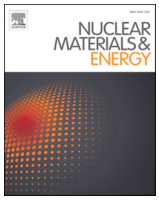

In-vessel and depth-resolved semi-quantitative analysis on hydrogen isotopes and wall materials in JET by LIBS operated on a remote handling arm☆

Rongxing Yi [a,*], Rahul Rayaprolu [a], Jari Likonen [b], Salvatore Almaviva [c], Ionut Jepu [d], Gennady Sergienko [a], Anna Widdowson [d], Nick Jones [d], Sahithya Atikukke [e], Timo Dittmar [a], Juuso Karhunen [b], Pawel Gasior [f], Marc Sackers [a], Shweta Soni [e], Erik Wüst [a], Jelena Butikova [g], Wojciech Gromelski [f], Antti Hakola [b], Indrek Jõgi [h], Peeter Paris [h], Jasper Ristkok [h], Pavel Veis [e], Sebastijan Brezinsek [a,i], UKAEA RACE Team

[a] Forschungszentrum Jülich GmbH, IFN-1 Plasma Physics, Jülich, Germany
[b] VTT Technical Research Centre of Finland Ltd., Espoo, Finland
[c] ENEA, Diagnostics and Metrology Laboratory, Frascati, Italy
[d] United Kingdom Atomic Energy Authority, Culham Campus, Abingdon, UK
[e] Comenius University, Faculty of Math, Physics and Informatics, Bratislava, Slovakia
[f] Institute of Plasma Physics and Laser Microfusion, Warsaw, Poland
[g] Institute of Solid State Physics, University of Latvia, Riga, Latvia
[h] University of Tartu, Institute of Physics, Tartu, Estonia
[i] HHU Düsseldorf, Faculty of Mathematics and Natural Sciences, Düsseldorf, Germany

A B S T R A C T

The tokamak JET achieved a groundbreaking milestone in nuclear fusion during its final deuterium–tritium experimental campaign (DTE-3) by setting a new world energy record [1]. To investigate in-vessel the fuel retention and wall material migration in JET post DT operation and clean-up phase with baking and glow discharge cleaning, a laptop-sized laser-induced breakdown spectroscopy (LIBS) system was deployed and mounted on a remote handling arm inside JET. The 800 ps (10 mJ) laser (wavelength 1064 nm) achieved a spatial and depth resolution of 130 μm and 180 nm on tungsten plasma-facing components (1000 pulses), respectively. Over 800 positions including beryllium first wall and tungsten divertor were studied by LIBS and provided both the spatial distribution and depth profiles of retained hydrogen (H) isotopes. LIBS spectra from four spectrometer systems enabled both high-resolution, high-sensitivity measurements and a broad spectral range simultaneously. Among them, a high throughput and high spectral resolution spectrometer in Littrow-arrangement was applied to distinguish the hydrogen isotopes. This in-vessel analysis demonstration provides vital information about the applicability of the technique for retention studies in future fusion reactors.

1. Introduction

In the field of nuclear fusion research, plasma-wall interaction (PWI) is one of the most relevant topics to be studied in view of the viability of a fusion device and reactor. Critical PWI processes like fuel retention by implantation and co-deposition as well as erosion and deposition (migration) of plasma-facing materials (PFM) can lead to operational issues and challenges for safety. Fuel retention and erosion/deposition of PFM are key aspects in identifying suitable material for the first wall in a reactor like ITER [2,3]. Therefore, comprehensive research has been performed in the last decades to identify suitable methods to quantify fuel retention and the erosion/deposition of PFM. Many ex-situ methods, such as Rutherford Backscattering Spectrometry (RBS) [4,5], Nuclear Reaction Analysis (NRA) [6], Glow Discharge Optical Emission Spectroscopy (GD-OES) [7], LIBS [8] etc. are widely and successfully used for analysis. However, these ex-situ methods carry the risk of sample contamination by e.g. oxygen and water, transportation challenge due to radioactivity (e.g. Tritium), toxicity (e.g. Beryllium) and a potential influence of time on the sample properties (e.g. outgassing), all of which arise from the process of removing the samples from the machine. The most attractive to study PWI processes post-plasma operation is an in-operando or in-vessel method, which avoids extraction,

☆ This article is part of a special issue entitled: 'PFMC-20' published in Nuclear Materials and Energy.
* Corresponding author.

https://doi.org/10.1016/j.nme.2025.102016
Received 25 July 2025; Received in revised form 2 October 2025; Accepted 21 October 2025
Available online 22 October 2025

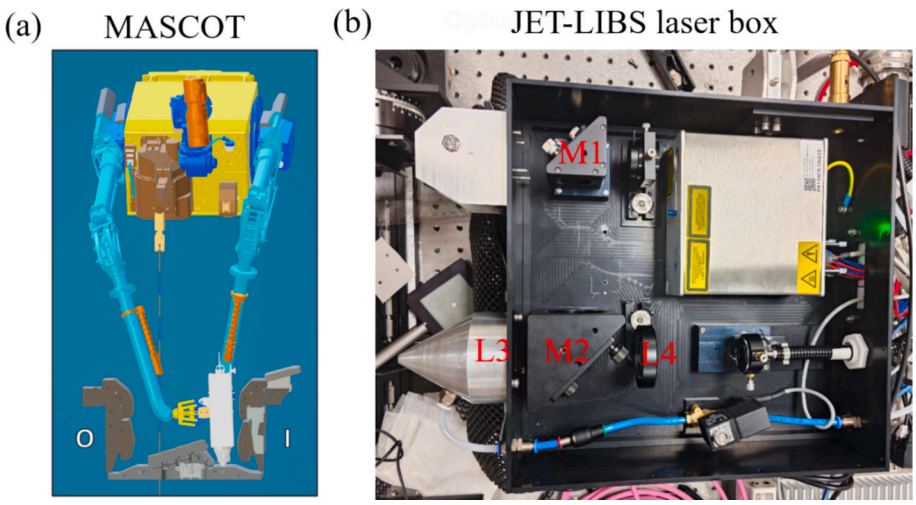

Fig. 1. (a) Diagram of MASCOT, O and I indicating outer and inner divertor, (b) setup of JET-LIBS laser box.

contamination, transportation, and can be timely carried out after the experiment. This will become even more relevant for PFMs installed in large fusion devices operating with DT or using actively cooled components. Laser-based techniques for surface analysis offer such capabilities, including methods based on desorption or ablation of materials [9]. In order to provide depth resolution, LIBS comes into the spotlight under these requirements and has been implemented in different fusion devices, pioneered as an in-situ technique in TEXTOR.

In TEXTOR, ns ruby and Nd:YAG lasers were applied to ablate graphite and tungsten limiters in-situ with a scanning mirror system. Carbon and hydrogen emission lines were spectroscopically observed from a millimetre-size spot on the limiter, proving the feasibility of using remote LIBS in fusion devices [10,11].

In EAST, about a decade later LIBS was also in-vessel applied. A ns Nd:YAG laser was utilised as an ablation source, along with a scanning mirror system. An area of 120 × 120 mm^2 on the high field side of the first wall could be analyzed by LIBS [12,13]. These mirror-based (remote) LIBS systems can be operated between or during plasma operations without harming the vacuum integrity. However, due to the limited size of the observation window, only a small area of the first wall can be detected, which significantly affects the detection sensitivity, especially for hydrogen isotopes as those are typically retained in low concentrations in the atomic percentage range.

The successful implementation of remote LIBS in TEXTOR and EAST proved the in-situ fuel retention and material erosion/deposition detection capability of LIBS. However, the limitation of detection area and low sensitivity are two principal drawbacks of this approach, which are limited to only a fraction of the PFCs in the vessel. LIBS positioned on a remote handling arm system becomes a viable alternative option to cure the limitations of mirror-based (remote) LIBS.

A compact double pulse ns LIBS system mounted on a robotic arm was developed and performed LIBS measurements inside the FTU tokamak on the overall vacuum vessel wall. With a two-spectrometer system (full range spectrometer and high resolution one), wall material like Mo and Al can be observed, but H and D peaks cannot be separated well due to the high content of H as the analysis was conducted in air long after plasma operation. (results from ex-situ show separated H and D peaks) [14,15].

All the continuous in-situ LIBS investigations over the past decade have given confidence to apply the technique in JET post-DT operation in a controlled area, with radioactive fuel, and toxic wall material. Information is gained shortly after the operation in contrast to ex-situ analysis which typically take place years after end of operation in a limited number of laboratories with the required licensing to handle those materials. To study the depth distribution of retained fuels and material composition, while avoiding the influences of sample contamination, radioactivity (T), and toxic sample (Be), a specially designed JET-LIBS system has been designed, built, and mounted on a remote handling arm system and deployed inside the JET vessel. A comprehensive introduction to the JET-LIBS project can be found in this paper [16]. The JET-LIBS system uses an ultra-short sub-ns laser to reduce thermal effects causing diffusion of fuel in the PFM and makes qualification of fuel retention from the interaction volume more suitable (less thermal effect, less outgassing from the adjacent layer). A suite of spectrometer systems which complement each other give access to material composition and fuel retention with either high spectral coverage, high spectral resolution, high sensitivity or high time resolution. Here, we focus on a custom-made Littrow spectrometer with large entendue [17] that can give higher sensitivity for H isotope separation analysis. Furthermore, owing to the high manoeuvrability of the remote handling arm system, it can perform near-comprehensive detection of the JET vessel with all relevant vessel components with a lateral resolution down to 1 mm. During the LIBS measurement campaign, over 800 positions were investigated in the W divertor and Be limiter area under Ar atmosphere, providing both spatial distribution and depth profiles of retained H isotopes after the complex post-DT clean-up phase in JET.

Table 1
Details of spectrometers.

Spectrometer	Company	Range (nm)	Resolution (nm)	F-number
Aryelle 200	LTB	260–760	~0.08	10
Avantes AvaSpec-ULS2048CL	Avantes	300–1100	~1	/
Littrow	FZJ	654–658	~0.03	5.9
SiPMs + filters	FZJ	on filter	/	/

2. Experimental method

2.1. Experimental setup

The JET-LIBS system mainly consists of 2 parts, the LIBS system and the remote handling arm system. The remote handling arm system (MASCOT) has been developed and operated by the UKAEA RACE Team (see Fig. 1(a)). It is a two-armed machine with back-drivable actuators and a large dexterous workspace in which each arm can operate within the full six degrees of freedom, providing a whole vessel detection capability [18].

The LIBS setup includes a Nd: YAG laser (pulse duration: 0.8 ns,

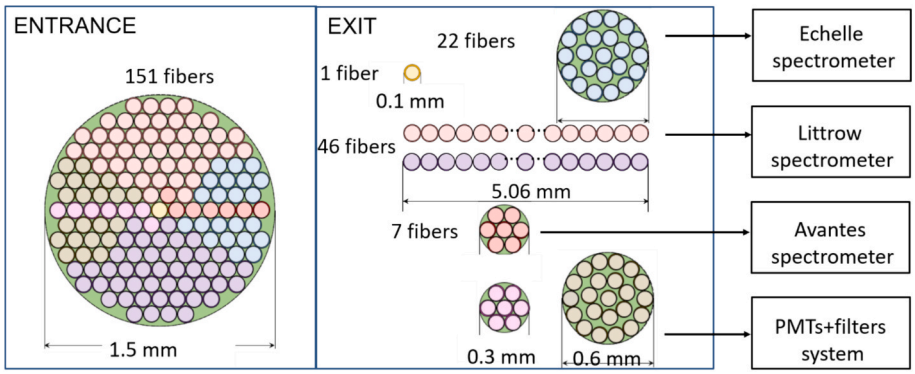

Fig. 2. Diagram of the fiber bundle and multi-spectrometer system.

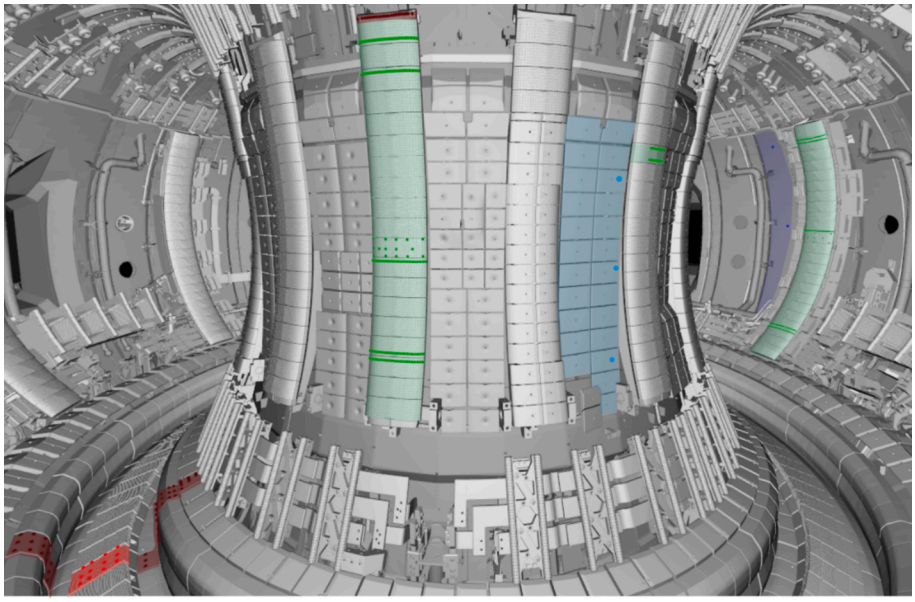

Fig. 3. PFCs measured in the JET-LIBS campaign. The red region in the divertor (module 2) represents the bulk-W tile 5 lamella and the W-CFC. The green region is bulk Be and the blue region is Be coated Inconel. (For interpretation of the references to colour in this figure legend, the reader is referred to the web version of this article.)

frequency: 2 Hz, wavelength: 1064 nm, pulse energy: 10 mJ, Montfort Laser M−Nano laser), 4 spectrometers (details in Table 1), and a 20 m fiber connecting the LIBS laser box and terminating through a multi-channel fiber bundle for the individual spectrometers. In Fig. 1 (b), the compact laser is fixed in the JET-LIBS laser box. The laser is reflected by mirror 1 (M1) and dichroic mirror 2 (M2) (both at 45°), then focused at a distance of 65 mm in front of lens 3 (L3) (75 mm focal length). A metal cone is used to precisely maintain the 65 mm distance and keep a local Ar ambient. Lens 4 (L4) collects plasma light into the 20 m fiber (1.5 mm diameter), which is then terminated into the multi-channel fiber bundle, and finally delivers plasma light to the 4 spectrometers, respectively (as shown in Fig. 2). An Aryelle 200 Echelle-type spectrometer is connected to a 0.6 mm fiber bundle, the Littrow spectrometer is connected to a linear fiber bundle, the Avantes spectrometer is connected to a 0.3 mm circular fiber bundle and a set of silicon photomultipliers (SiPMs) equipped with narrowband interference filters connected to 2 fiber bundles (0.3 mm + 0.6 mm). Details about the 4 spectrometers are described below and in Table 1:

1. The Aryelle 200 has lower sensitivity but a wide wavelength range and high spectral resolution. It is used to collect plasma light in the early stage of the plasma (short delay time), when the electron density remains high enough to satisfy local thermodynamic equilibrium (LTE). Calibration-free LIBS (CF-LIBS) will be performed using these spectra for quantitative analysis and will be reported in upcoming publications
2. The Avantes (AvaSpec-ULS2048CL) has only 1 nm resolution but a wide wavelength range. It is used to collect whole lifetime plasma light (no time resolution) from the visible to near-infrared region, where most spectral lines of the PFM can be observed [19]
3. The Littrow spectrometer is a custom-made device with a large grating size (165 × 135 mm, 1200 l/mm) and a 750 mm focal length, works in 2nd order, resulting in high sensitivity and resolution. It is coupled with an Andor USB iStar camera (A-DH334T-18F-A3) to capture H_α and its isotopes' lines [20]
4. The SiPMs + filters system is an additional custom-made spectrometer. It has two fiber interfaces. The first interface, three filters with different bandwidths (656.2 ± 1.74 nm, 656.6 ± 3.78 nm, 656.5 ± 8.65 nm) are connected to three SiPMs (SPMMini3000X03A1), respectively. It has been mentioned here for completeness, but no further analysis is shown

All the spectrometers were placed outside of the JET vessel, with only the box shown in Fig. 1 being installed inside the vessel.

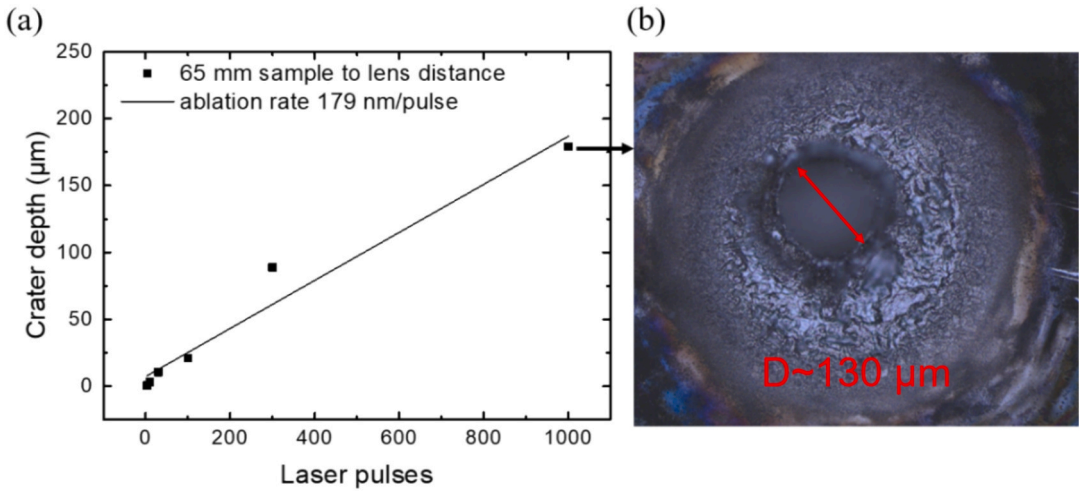

Fig. 4. (a) Crater depth vs. number of laser pulses on pure W using the JET-LIBS setup providing the ablation rate. (b) Image of the ablation crater after 1000 laser pulses.

2.2. Measured positions

Out of the 840 positions from the whole inner vessel, 20 positions were measured in the tungsten divertor module 2 (see Fig. 3), which is the focus of this publication. Repetitive laser pulses ranging from 100 to 1500 pulses were shot at each position, providing depth-resolved information for retained fuel and material composition. W-coated carbon-fiber composite (CFC) tiles with a W/Mo/CFC layer structure are the main original materials in the divertor, with the load-bearing septum replacement plate (LBSRP) in tile 5 being bulk-W. Be is the main material at limiters and vessel wall areas and it migrates by PWI processes towards the divertor causing erosion and deposition [21]. All planned LIBS analysis components are shown in Fig. 3, with the specifically analyzed divertor area marked in red in this paper, including the High Field Gap Closure (HFGC), which is known from earlier ex-situ analysis to show the largest Be deposits and highest fuel content resulting from material migration [22].

3. Results and discussion

3.1. Laser ablation characteristics

In order to optimise and calibrate the LIBS system regarding delay time, and to determine the ablation rate for bulk-W before the actual in-vessel measurements in JET, a polished bulk-W sample (Plansee comparable to JET bulk-W) was exposed in a laboratory arrangement to various laser pulses. As depicted in Fig. 4, the average ablation rate on this grade of W is about 180 nm/pulse considering 1000 consecutive laser pulses and crater analysis by profilometry (Dektak 6 M, Veeco Instruments). The diameter of the laser ablation crater amounts approximately 130 µm. With a laser energy of 10 mJ per pulse the laser fluence can be calculated to be around 75.4 J/cm^2.

3.2. Spectral analysis

The analysis of the spectral data recorded with the Littrow spectrometer and the Avantes spectrometer will be presented in this section, while the results from the Aryelle spectrometer can be found in the adjacent paper [23].

3.2.1. Littrow spectrometer

The custom-made spectrometer in Littrow arrangement in this work is used for H isotope analysis. H spectrum is very sensitive to plasma electron density, resulting in significant Stark broadening at high electron densities [24,25]. Therefore, it is important to find a suitable delay time with low electron density to detect the spectrally separated H isotopes (Balmer-alpha lines, 3 > 2 transition) around 656 nm. Reference W-coated CFC samples (WEST and JET [16]) were exposed by the laser

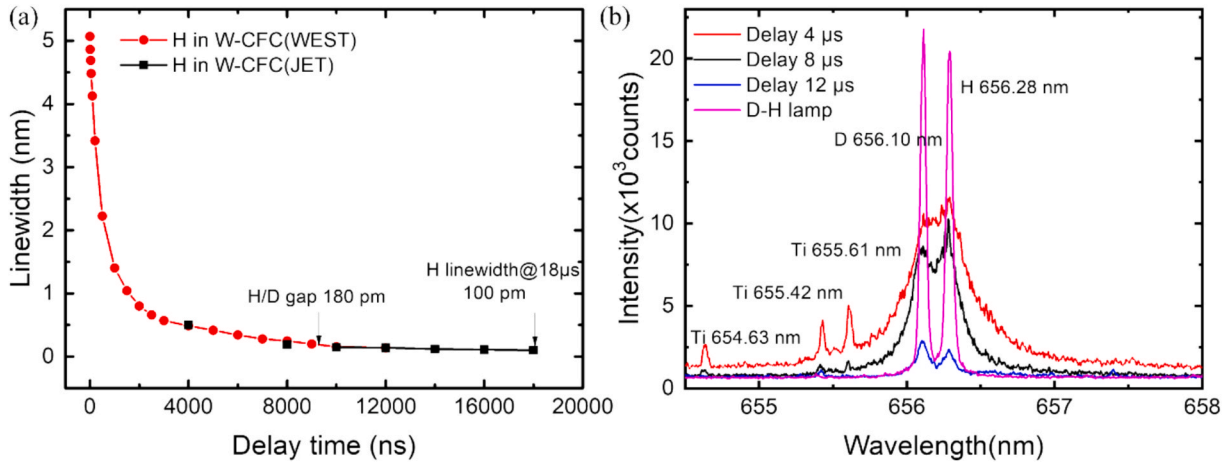

Fig. 5. (a) Influence of delay time between laser impact and detection on the linewidth of H Balmer-alpha, (b) Typical spectra of the H isotopes at delay times of 4, 8, 12 µs from the JET W-CFC sample. A reference spectrum from a D-H low-pressure lamp is shown for comparison.

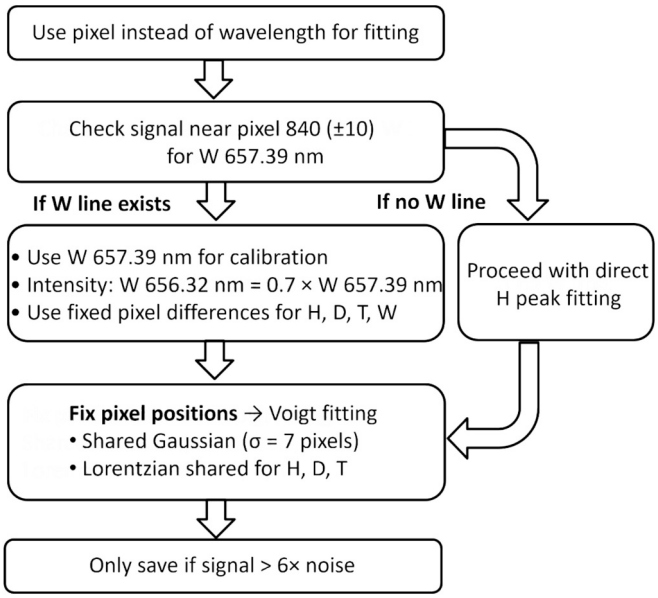

Fig. 6. Flowchart for fitting Littrow spectral data.

to optimize the delay time of the LIBS plasmas, with each delay time tested in a fresh position on the samples.

As shown in Fig. 5 (a), red data points represent the WEST sample, and black data points represent the JET sample. Both samples show a similar trend. As the delay increases, the linewidth of hydrogen Balmer alpha decreases rapidly, reaching 180 pm at 8–9 μs, which is theoretically sufficient to resolve the Balmer-alpha H and D spectral lines (isotope shift 0.18 nm). It then slowly decreases to 0.10 nm at 18 μs, still higher than the isotope shift between D and T (isotope shift 0.06 nm). However, the spectral intensity of D also decreases very quickly with increasing delay time, therefore the experiment was stopped at 18 μs. A delay time of 8–12 μs was chosen as the standard setting for the in-vessel experiments to ensure sufficient separation between the H and D peaks while retaining as much retention information as possible from the deposited layer. Typical spectra from JET W-CFC samples analysis at delay times of 4, 8 and 12 μs are shown in Fig. 5 (b). The D in H shoulder can be distinguished even at delay times of 4 μs when the H linewidth is around 450 pm, but it is only visibly separated at 8 μs, and even better at 12 μs with lower intensity.

Most spectra obtained in our measurement contain W I and Ti I lines, the origin of Ti potentially comes from the Ti coil in JET [26]. With the interference of W and Ti lines located around the H line, the only way to extract H, D and even T signals is through spectral fitting. However, the fitting result is easily affected by the initial peak position, which had a six pixels deviation during the two weeks analysis campaign due to temperature variations in the JET torus hall. An empirical fitting strategy as shown below has been introduced to enhance the fitting reliability, as shown in Fig. 6.

Based on this strategy, fitting results of the four types of spectra are shown in Fig. 7. Fig. 7 (a) shows the spectra from the outer divertor apron (tile 8, see Fig. 8(c)). This location is known from post-mortem analysis of tiles from earlier campaigns to have no Be deposition, but rather intact W-coated CFC surfaces. In addition to the H isotopes lines, spectral lines of W are also visible. The fitting R^2 is 0.9630 due to the ignoring of the three small W I lines, which have no influence on the H isotopes. Fig. 7 (b) shows the corresponding spectra from the HFGC tile located at the apron of the inner divertor and known from previous studies to be deposited by Be. The appearance of the Ti I line has replaced the W I lines. The fitting R^2 is 0.9871. The broad spectral tail beside the Ti I line influences the result, especially when the hydrogen signal is low. Pure H isotopes lines appear in the spectrum shown in

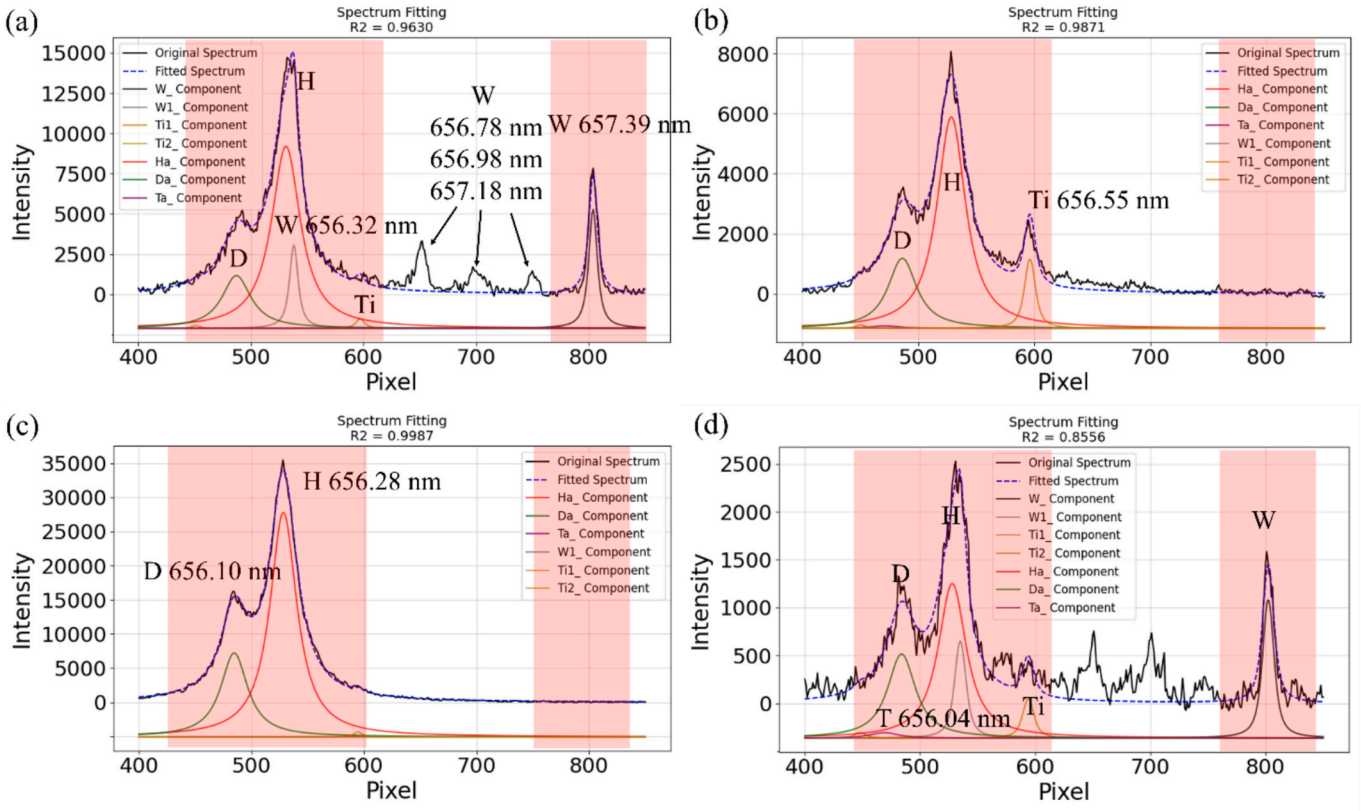

Fig. 7. (a) Fitting results of outer divertor tile 8 at position 18 pulse 31, (b) Fitting results of inner divertor HFGC tile at position 1 pulse 13, (c) Fitting results of inner divertor HFGC tile at position 2 pulse 8, (d) Spectral of divertor tile 4 at position 11 pulse 17.

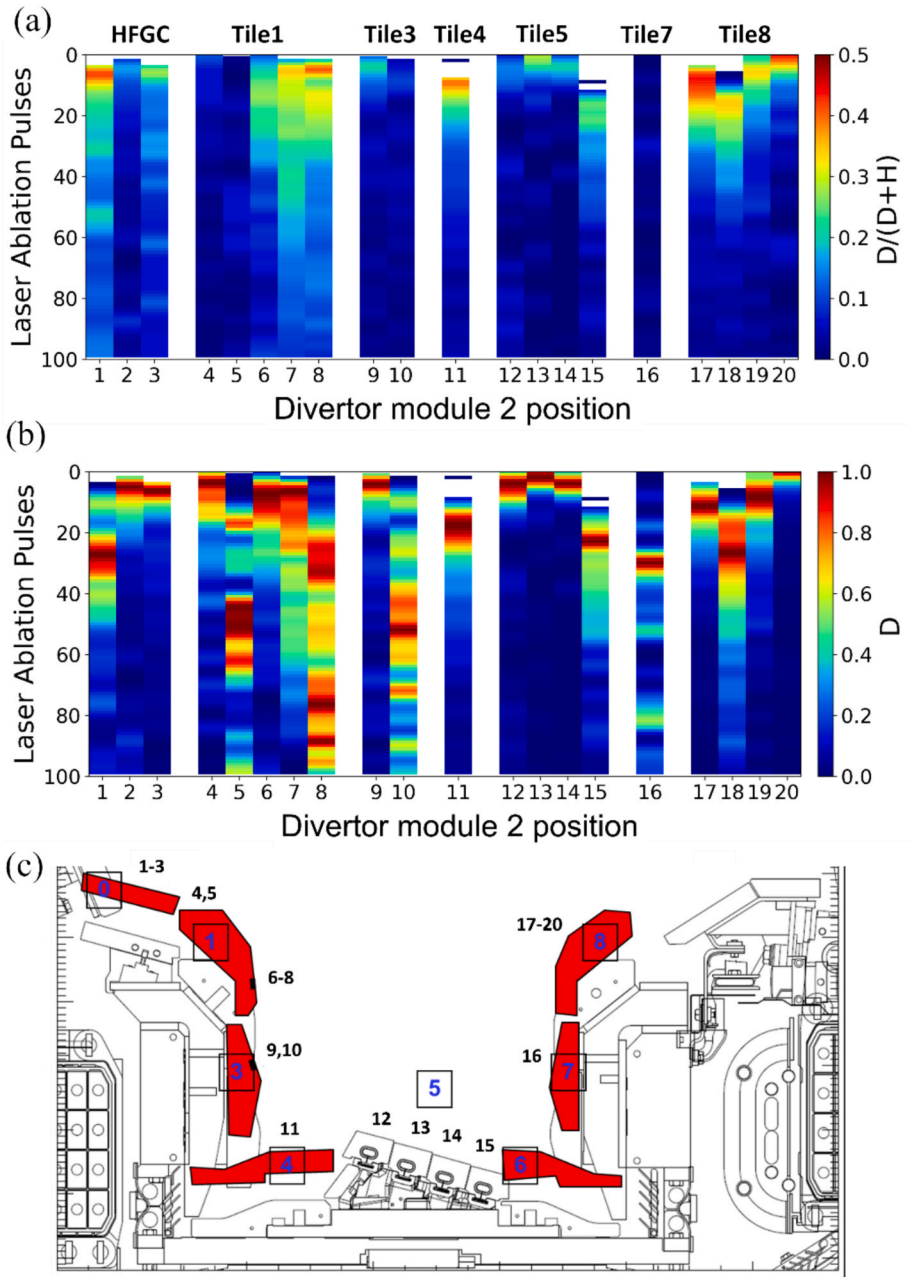

Fig. 8. (a) Depth and poloidal distribution of the D/(H + D) ratio in the W divertor (module 2), (b) Depth and poloidal distribution of the D alpha emission in the W divertor, (c) Poloidal cross-section of the JET tungsten divertor with tile nomenclature and LIBS measurement locations.

Fig. 7 (c), which was also recorded at the HFGC, but at a slightly different poloidal position, the fitting R^2 is 0.9987, which indicates a very reliable fitting result. The fitting results show that significant D signals exist in the whole divertor area. An example of the T fitting is shown in Fig. 7(d). The signal level is very low and uncertainties in the fitting procedure are high. Considering that the noise signal is about one percentage of the deuterium signal and the tritium intensity is almost at the noise level, the tritium signal might contribute to the percentage range. Improvements in the fitting procedure and analysis of individual spectra are ongoing to provide an upper limit of the T isotope concentration, but this is outside of the present paper.

Fig. 8 (a) and 8 (b) show the depth profile and the poloidal distribution of (a) the isotope ratio of D/(H + D) based on the described line analysis of Balmer lines and (b) the D intensity normalised to the maximum value measured in the JET W divertor in poloidal module 2. 100 LIBS measurement points have been taken at one spatial position. The studied spatial positions are indicated in the poloidal cross-section of the divertor in Fig. 8 (c). Note, that the first 100 pulses might, in the presence of very thick layers as present at the HFGC tile, be insufficient to cover the total content, thus, the information here shall give a first insight in the depth and poloidal distribution. Moreover, the origin of the detected D is in the present case caused by a mixture of co-deposition and deeper implantation. The near surface coverage and implantation of D is mostly absent due to the short lifetime (only visible before 6 μs) of the Balmer-line in the loose surface layer. The white bars in the first pulses, therefore the first 100 s of nm, underline this (indicates a very loose surface layer). Tritium is almost absent and undetectable due to the post DT cleaning activities in the JET vessel. The concentration is so low, that it is – if present – a contribution below the percentage range in the D signal (see in Fig. 7 (d)). Therefore, the plots refer only to the D/(H + D) ratio and not the total ratio of D/(H + D + T). The isotope ratio can be quantified even without absolute calibration of

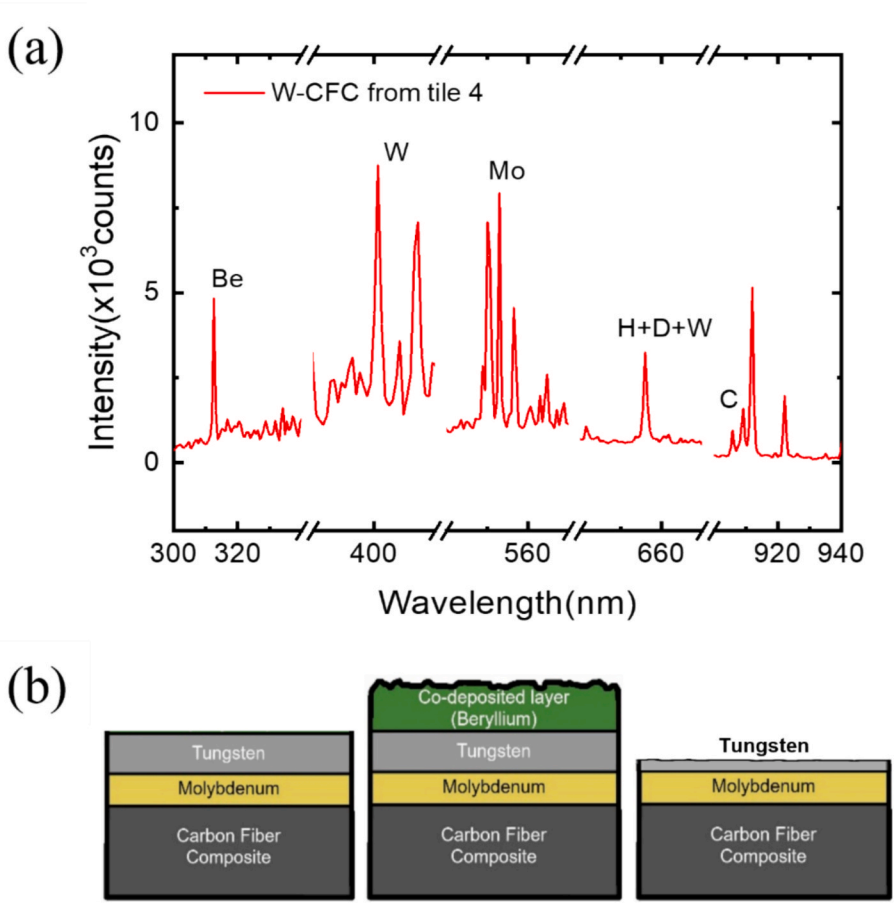

Fig. 9. (a) Spectra of Be, W, Mo, Balmer-alpha + W and C from tile 4 in the divertor module 2, as well as (b) the typical W-CFC structure in JET.

the LIBS signal as no change in sensitivity is expected, and the atomic data for excitation of the observed Balmer-line for the different isotopes are comparable. In contrast, the total content of the fuel in the plasma-facing material or deposit, thus the material composition, require either CF-LIBS or reference samples for calibration (see 3.3). CF-LIBS is foreseen by using the Aryelle spectrometer treating the hydrogen isotopes as one element. The results from the Littrow spectrometer will then provide the hydrogen isotope composition, which needs to be folded with the total hydrogenic contribution.

3.2.2. *Avantes spectrometer*

The compact overview spectrometer with a wavelength span from the near UV to the near IR-range is most suitable to study simultaneously the fuel species and multiple impurity species ablated from the plasma-facing components. This allows the study of material migration in JET, thus the erosion, transport and deposition of the main plasma-facing materials W (divertor) and Be (main chamber), as well as integrated information about the hydrogenic fuel content. The hydrogen isotopes cannot be spectrally resolved with the system. Fig. 9 (a) shows the typical spectrum recorded with the system and the main lines studied indicated: Be 313.1 nm, W 400.9 nm, and the unresolved W 656.3 nm plus Balmer-alpha at 656.1 /656.3 nm of D and H. Moreover, the lines of Mo 553.3 nm and C 906.2/909.5 nm can typically be detected in depth when applying LIBS to the W-coated CFC tiles in the divertor.

Fig. 9 (b) shows schematically the three situations which can appear on the W-coated CFC tiles. Left: the original structure with about 20μm W coating on a thin (4–5 μm) Mo-interlayer deposited on the CFC base structure. Middle: the typical situation in a deposition zone with Be deposited on top of the W coating. Right: the typical situation of an erosion zone with the initial W-coated surface partially or fully eroded. The Mo interlayer was initially applied to better matching of the thermal expansion coefficient between the W coating and the CFC substrate, but in the LIBS studies, the Mo is a unique depth marker, functioning similarly to the C in the substrate. A critical point in the depth analysis is the surface roughness of the substrate and the Mo interlayer, in μm-range during production. The laser interaction area is significantly larger than the roughness, thus it averages substantially. However, the Mo marker-layer zone is still wider than the actual layer thickness. Additionally, matrix effects and an imperfect laser profile smooth against the width, thus, the most significant information is the first appearance of Mo and C as depth information. In combination with the appearance of Mo transported originally from the main chamber into the divertor and the remaining W signal, a footprint of the averaged erosion and deposition pattern in the JET divertor can be obtained. The averaging is over the exposure time, magnetic configurations applied, and the associated plasma conditions.

The characteristic line emission of the five strongest lines of W, Be, Mo, C and (H + D + W) atoms mentioned above was used to provide an initial depth profile analysis at the surface of the W divertor at the end of JET operation. At this stage the depth scale refers to the number of laser pulses and needs in future to be carefully converted into μm. In particular the ablation rate in different material zones like Be deposits or e.g. bulk W will differ, but the obtained information from the measurements is suitable for a qualitative interpretation.

In Fig. 10 is the material composition along the poloidal measurement points (Fig. 8 (c)) in module 2 of the JET divertor depicted by visualisation of the main line emission: (a) Beryllium measured at Be I 313.1 nm, (b) Tungsten measured at W I at 400.9 nm, (c) Molybdenum measured at Mo I at 554.3 nm, (d) Carbon measured at C I at 908.6 nm, and (e) the unresolved W I and Balmer-alpha line of hydrogen isotopes at

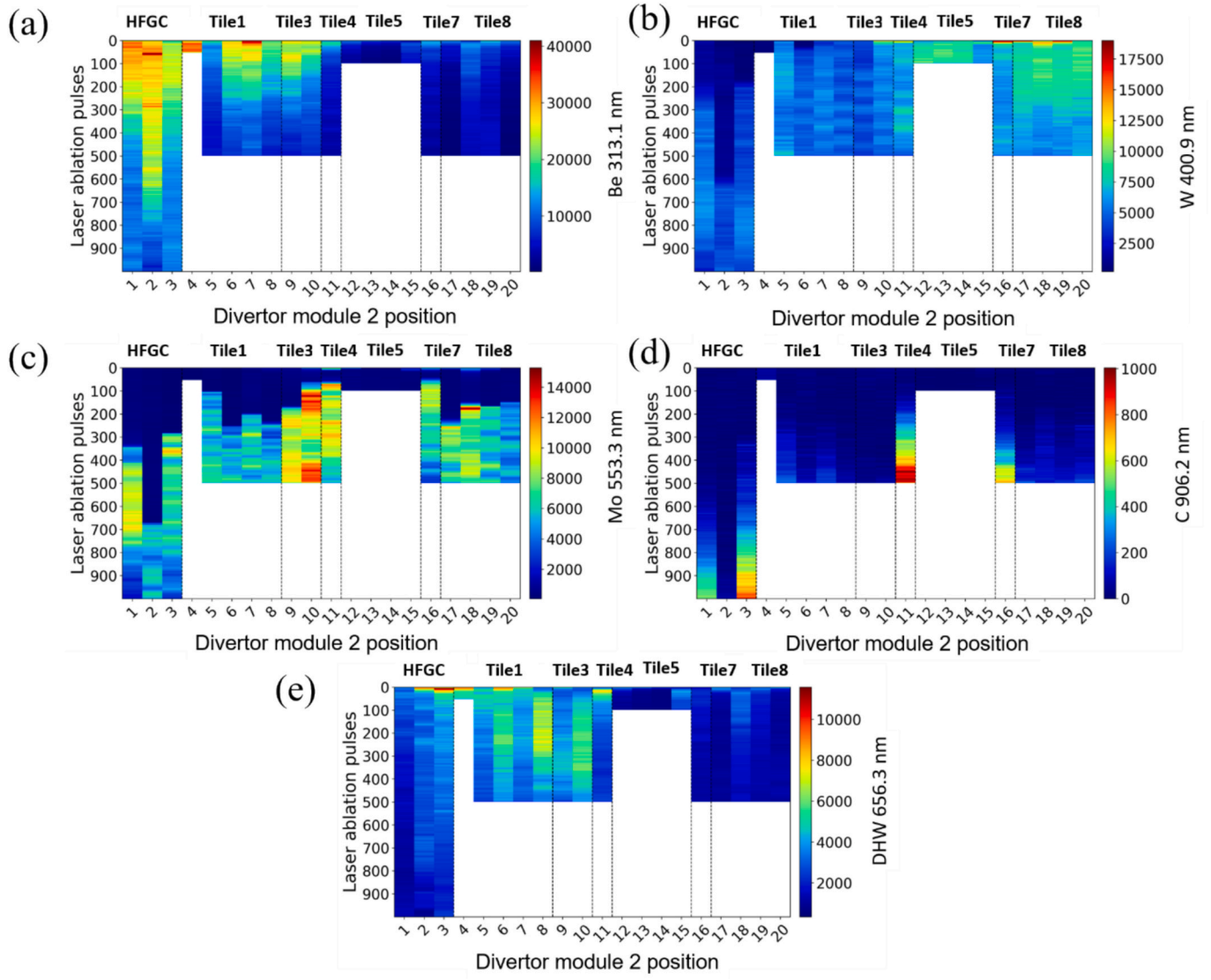

Fig. 10. Depth and poloidal distribution of (a) Be 313.1 nm, (b) W 400.9 nm, (c) Mo 553.3 nm, (d) C 906.2 nm and (e) H + D + W 656.3 nm in the divertor module 2 area.

656.3 nm. A number of key characteristic features can be identified at a first glance. Comparing the Be and W pattern, it is clear that the inner divertor (HFGC, tile 1, tile 3) represents a strong deposition zone with thick Be layer. The outer divertor (tile 5, tile 7 and tile 8) shows no relevant Be layer growth. A tungsten surface can be observed on these tiles of the divertor from almost the first laser pulse.

The strongest erosion is in the accessible area of tile 4 and the lower part of tile 7. Note there was no access to tile 6 with the LIBS system. Tile 4 and tile 6 were the locations of the inner and outer strike line in the majority of pulses in high performance. The lower part of tile 3 and tile 7 are in the near scrape-off layer and see also some erosion. In these cases, the Mo marker layer is reached very quickly at around 60 pulses, indicating that the residual W-coating was almost fully eroded at the end of JET operation. Moreover, at these locations also C appears soon in the spectrum after a few hundreds of pulses. This confirms the strong net erosion in these places. In contrast, no C is seen in the other locations in the first 500 pulses and Mo appears typically at around 200 pulses in the outer divertor. The Mo line only appears occasionally on the surface (the initial few pulses, see tiles 4, 7 and 8) due to slight implantation or co-deposition from a source potentially on tile 6 or lower part 7, and the internal interface between W and Mo is quite sharp and clear. Therefore, the laser pulse number of the W/Mo interface is in future suitable for calculating the net deposition and erosion rate with the initial layer thickness. A comparison with an unused W-coated CFC will be used as secondary standard. The detection of the C I line at 909.6 nm even in the strong deposition zone of Be after 900 pulses confirms the capability of LIBS to perform deep depth analysis. Considering earlier analysis by Widdowson et al. [27,28] with other ex-situ techniques, the location of C shall be at least 45 μm below the top surface of the HFGC tile.

Lastly, the D 656.1 nm, H 656.3 nm, and W 656.3 nm lines are integrated into a single 656.3 nm line in the Avantes system. The intensity distribution of this 656.3 nm line shows no correlation with the W 400.9 nm line but exhibits a strong correlation with the Be 313.1 nm line from tile 1 to tile 4. Thus, co-deposition is here the main mechanism in the outer leg, very little fuel can be observed closer to the surface and is likely related to implantation. The unexpected reduction of the H + D signal observed in the HFGC area may be attributed to a poor adhesion or porosity of the co-deposition layer or effective cleaning.

3.3. *Semi-quantitative analysis of the retained fuel composition*

Before the lengthy process of analyzing the large amount of data by the CF-LIBS method with the Aryelle spectrometer data, a semi-quantitative analysis can be performed with the Littrow data using a

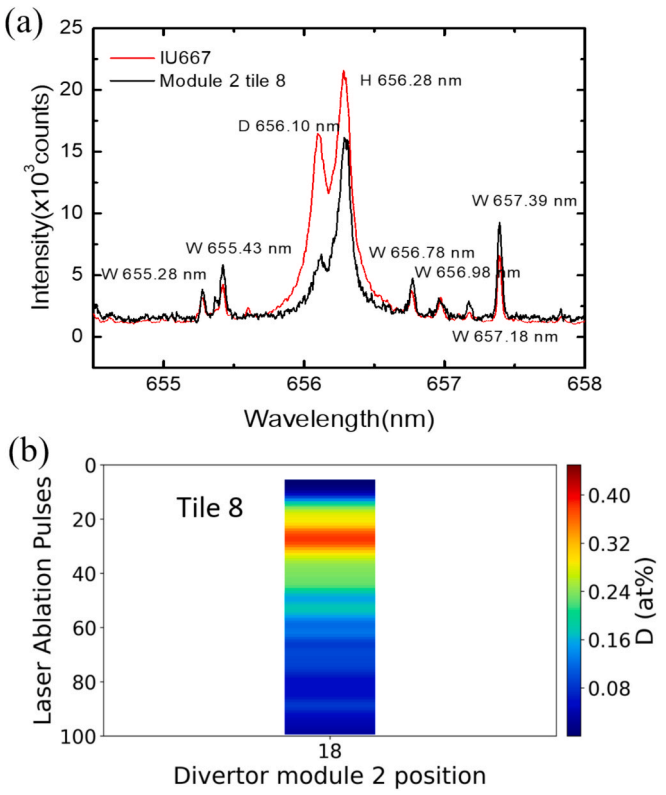

Fig. 11. (a) The LIBS spectra of IU667, module 2 divertor tile 8 (position 18). (b) Semi-quantitative result of D retention in tile 8 (position 18).

reference sample (IU667), a Mo substrate coated with a 5 μm W layer. The W coating was deposited by magnetron sputtering at the National Institute for Laser, Plasma & Radiation Physics (INFLPR), Romania. Ion implantation was subsequently carried out in the linear plasma device PSI-2 [29]. With the same JET-LIBS setup, IU667 was measured in the lab under the same laser and set-up parameters, and the retained D in IU667 was measured by Nuclear Reaction Analysis (NRA) in FZJ as a reference. NRA results show 2 at% D in the W coating of IU667.

Here, position 18 from the W-coated CFC tile 8 was chosen to do semi-quantitative analysis. LIBS spectra of IU667, of the divertor tile 8 (position 18) are shown in Fig. 11 (a). The semi-quantitative estimation of deuterium content was performed by calculating the integrated area ratio between the Dα line and the W I 657.39 nm line. IU667 with a known D concentration of 2 at% from NRA was used to establish the baseline. In tile 8, retention in the initial 7 pulses is undetectable due to the much shorter lifetime of H isotopes and the cleaning activities on this tile, after which D concentration gradually increases to a maximum of 0.5 at%, and then slowly decreases to 0.1 at% by the 100th laser pulse. By accumulating the D signal from the initial 100 laser pulses, about 1.5×10^{17} D/cm^2 exists in the divertor tile 8 area (assuming 179 nm/pulse ablation rate and ignoring the initial 7 empty pulses, which correspond to a 1.3 μm surface layer).

Furthermore, the limit of detection (LOD) for D was estimated to be approximately 0.07 at%, based on the average Dα signal intensity obtained from a 2 at% D reference sample (IU667) over laser pulses 2–12, and applying the 3σ criterion (three times the noise level). Given the similar spectral behavior of H isotopes and the comparable matrix effects in tungsten, it is reasonable to assume that T exhibits a similar LOD under the same conditions.

4. Conclusions

As the first in-vessel LIBS campaign on a fusion device that has undergone deuterium–tritium (D-T) reactions, this work proved that multi-output fiber bundles combined with multiple spectrometers for LIBS can effectively provide both high spectral resolution and wide spectral coverage simultaneously. This makes JET-LIBS setup able to detect the depth profile of H and D as well as the material composition semi-quantitatively. High D/H ratios appeared in the inner divertor area, and Ti deposition was observed for the first time in the JET HFGC area. Semi-quantitative results show 10^{17} D/cm^2 retention in the divertor tile 8, and the LOD for D of JET-LIBS setup is about 0.07 at%. Meanwhile, with the help of a remote handling arm system, LIBS has the capability to diagnose across all first wall locations with a 180 nm depth resolution and detect depths up to 200 μm.

While the accomplishments are important, it is equally important to reflect on the knowledge and experiences we have gained. Considerable experience was accumulated in the implementation of this system. First of all, H isotope signals by LIBS will disappear with the commonly used long delay times, which means a trade-off between fitting accuracy and loss of surface data. Secondly, to resolve T from D peak visually and obtain a good LOD at the same time, a spectral intensity enhancement method should be developed for longer delay times. Furthermore, to maintain long-term consistency of wavelength positions, it is of great importance to develop a remote calibration method that enables routine calibration even when the instrument is located within a controlled area. Calibration represents the primary obstacle in both spectral fitting and CF-LIBS.

LIBS on the JET remote handling arm was overall successful and could reproduce the main features of erosion and deposition in the JET divertor observed by post-mortem analysis in previous campaigns. LIBS confirmed the thick Be deposition in the inner divertor, strong W erosion at the typical strike-line locations on tile 4 and at the bottom of tile 7, clean W-coated CFC surface at the upper part of the outer divertor. The W-coating was apart from the strike-point regions still intact and the Mo interlayer was barely detectable. Fuel retention by co-deposition in the inner divertor was detectable, whereas in the analysed outer divertor target plates mainly implantation is visible. Tritium observation was impeded by the cleaning procedures applied before the experiment. Nevertheless, detection of this isotope brings optimistic perspective. Analysis beyond this qualitative picture will follow in the near future.

CRediT authorship contribution statement

Rongxing Yi: Writing – review & editing, Writing – original draft, Validation, Software, Methodology, Formal analysis, Data curation, Conceptualization. **Rahul Rayaprolu:** Writing – review & editing, Validation, Formal analysis, Data curation. **Jari Likonen:** Writing – review & editing, Validation, Supervision, Project administration, Methodology, Investigation, Funding acquisition, Data curation, Conceptualization. **Salvatore Almaviva:** Writing – review & editing, Validation, Resources, Methodology, Data curation, Conceptualization. **Ionut Jepu:** Writing – review & editing, Validation, Resources, Data curation. **Gennady Sergienko:** Writing – review & editing, Validation, Resources, Methodology, Formal analysis, Data curation, Conceptualization. **Anna Widdowson:** Validation, Resources, Data curation. **Nick Jones:** Resources, Data curation. **Sahithya Atikukke:** Writing – review & editing, Data curation. **Timo Dittmar:** Data curation. **Juuso Karhunen:** Data curation. **Pawel Gasior:** Writing – review & editing, Data curation. **Marc Sackers:** Writing – review & editing, Data curation. **Shweta Soni:** Writing – review & editing, Data curation. **Erik Wüst:** Writing – review & editing, Data curation. **Jelena Butikova:** Data curation. **Wojciech Gromelski:** Writing – review & editing, Data curation. **Antti Hakola:** Data curation. **Indrek Jõgi:** Writing – review & editing, Data curation. **Peeter Paris:** Writing – review & editing, Data curation. **Jasper Ristkok:** Data curation. **Pavel Veis:** Writing – review & editing, Data curation. **Sebastijan Brezinsek:** Writing – review & editing, Writing – original draft, Validation, Supervision, Resources, Project administration, Methodology, Investigation, Funding acquisition, Data curation, Conceptualization.

Declaration of competing interest

The authors declare that they have no known competing financial interests or personal relationships that could have appeared to influence the work reported in this paper.

Acknowledgements

This work has been carried out within the framework of the EUROfusion Consortium, funded by the European Union via the Euratom Research and Training Programme (Grant Agreement No 101052200 — EUROfusion), from the EPSRC [grant number EP/W006839/1] and within the framework of the Contract for the Operation of the JET Facilities and has received funding from the European Union's Horizon 2020 research and innovation programme. Views and opinions expressed are however those of the author(s) only and do not necessarily reflect those of the European Union or the European Commission. Neither the European Union nor the European Commission can be held responsible for them. The research used UKAEA's Materials Research Facility, which has been funded by and is part of the UK's National Nuclear User Facility and Henry Royce Institute for Advanced Materials. This work was also conducted as part of an international project co-financed by the Polish Ministry of Science and Higher Education within the programme called 'PMW'.

Data availability

Data will be made available on request.

References

[1] EUROfusion. (Feb. 8, 2024). Breaking New Ground: JET Tokamak's Latest Fusion Energy Record Shows Mastery of Fusion Processes. [Online]. Available: https://euro-fusion.org/eurofusion-news/dte3record/.
[2] S. Brezinsek, T. Loarer, V. Philipps, Fuel retention studies with the ITER-Like Wall in JET, Nucl. Fusion 53 (2013) 083023.
[3] S. Brezinsek, A. Kirschner, M. Mayer, et el., Erosion, screening, and migration of tungsten in the JET divertor. Nuclear Fusion, 59(2019) 096035.
[4] M. Mayer, Rutherford backscattering spectrometry (RBS). Workshop on Nuclear Data for Science and Technology: Materials Analysis. Vol. 34. 2003.
[5] M. Mayer, M. Balden, S. Brezinsek, et al., Material erosion and deposition on the divertor of W7-X, Phys. Scr. T171 (2020) 014035.
[6] W.A. Lanford, Analysis for hydrogen by nuclear reaction and energy recoil detection, Nucl. Instrum. Methods Phys. Res., Sect. B 66 (1992) 65.
[7] C.N. Taylor, M. Shimada, First GD-OES results on various deuterium ion fluences implanted in tungsten, Nucl. Mater. Energy 16 (2018) 29.
[8] H.J. Meiden, S. Almaviva, J. Butikova, et al., Monitoring of tritium and impurities in the first wall of fusion devices using a LIBS based diagnostic, Nucl. Fusion 12 (2021) 125001.
[9] M. Zlobinski, G. Sergienko, I. Jepu, et al., First results of laser-induced desorption-quadrupole mass spectrometry (LID-QMS) at JET, Nucl. Fusion 8 (2024) 086031.
[10] N. Gierse, B. Schweer, A. Huber, et al., In situ characterisation of hydrocarbon layers in TEXTOR by laser induced ablation and laser induced breakdown spectroscopy, J. Nucl. Mater. 415 (2011) S1195–S1198.
[11] Q. Xiao, R. Hai, H. Ding, et al., In-situ analysis of the first wall by laser-induced breakdown spectroscopy in the TEXTOR tokamak: Dependence on the magnetic field strength, J. Nucl. Mater. 463 (2015) 911–914.
[12] Z. Hu, C. Li, Q. Xiao, et al., Preliminary results of in situ laser-induced breakdown spectroscopy for the first wall diagnostics on EAST, Plasma Sci. Technol 19 (2017) 025502.
[13] D. Zhao, C. Li, Z. Hu, et al., Remote in situ laser-induced breakdown spectroscopic approach for diagnosis of the plasma facing components on experimental advanced superconducting tokamak, Rev. Sci. Instrum. 89 (2018) 073501.
[14] S. Almaviva, L. Caneve, F. Colao, et al., LIBS measurements inside the FTU vessel mock-up by using a robotic arm, Fusion Eng. Des. 157 (2020) 111685.
[15] S. Almaviva, L. Caneve, F. Colao, et al., LIBS measurements inside the FTU vacuum vessel by using a robotic arm, Fusion Eng. Des. 169 (2021) 112638.
[16] J. Likonen, S. Almaviva, R. Rayaprolu, et al. this conference.
[17] S. Brezinsek, Untersuchung von atomarem und molekularem Wasserstoff vor einer Graphitoberfläche in einem Hochtemperatur-Randschichtplasma, Institut Für Plasmaphysik (2002) PreJuSER-25618.
[18] D. Hamilton and G. Preece, Development of the MASCOT Telemanipulator Control System, EFDA–JET–PR(01)06 report.
[19] D. Zhao, R. Yi, A. Eksaeva, et al., Quantification of erosion pattern using picosecond-LIBS on a vertical divertor target element exposed in W7-X, Nucl. Fusion 1 (2020) 016025.
[20] E. Wüst, T.S. Selinger, C. Kawan, et al., Depth-resolved deuterium retention analysis in displacement-damaged tungsten using laser-induced breakdown spectroscopy, Phys. Plasmas 8 (2024).
[21] S. Brezinsek, A. Widdowson, M. Mayer, et al., Beryllium migration in JET ITER-like wall plasmas, Nucl. Fusion 6 (2015) 063021.
[22] A. Widdowson, J.P. Coad, Y. Zayachuk, et al., Evaluation of tritium retention in plasma facing components during JET tritium operations, Phys. Scr. 12 (2021) 124075.
[23] S. Almaviva, J. Likonen, A. Hakola et al. this conference.
[24] H.R. Griem, A.C. Kolb, K.Y. Shen, Stark broadening of hydrogen lines in a plasma, Phys. Rev. 116 (1959) 4.
[25] I. Jõgi, J. Ristkok, J. Raud, Laser induced breakdown spectroscopy for hydrogen detection in molybdenum at atmospheric pressure mixtures of argon and nitrogen, Fusion Eng. Des. 179 (2022) 113131.
[26] K.D. Lawson, I.H. Coffey, F. Rimini, et al., Impurity analysis of JET DiMPle pulses, Plasma Phys. Controlled Fusion 63 (2021) 105001.
[27] A. Widdowson, J.P. Coad, E. Alves, et al., Deposition of impurity metals during campaigns with the JET ITER-like Wall, Nucl. Mater. Energy 19 (2019) 218–224.
[28] S. Krat, M. Mayer, A. Baron-Wieche, et al., Comparison of erosion and deposition in JET divertor during the first three ITER-like wall campaigns, Phys. Scr. T171 (2020) 014059.
[29] A. Kreter, C. Brandt, A. Huber, et al., Linear plasma device PSI-2 for plasma-material interaction studies, Fusion Sci. Technol. 68 (2015) 8–14.